2007 IEEE International Conference on
Robotics and Automation
Roma, Italy, 10-14 April 2007

Nanorobotic Spot Welding by Attogram Precision Metal Deposition from Copper-filled Carbon Nanotubes

Lixin Dong[1], *Member, IEEE,* Xinyong Tao[2], Li Zhang[1], *Student Member, IEEE,* Xiaobin Zhang[2], and Bradley J. Nelson[1,*], *Senior Member, IEEE*

***Abstract*—Nanorobotic spot welding using single-crystalline-copper-filled carbon nanotubes (CNTs) is investigated experimentally inside a transmission electron microscope (TEM). Controlled melting and flowing of copper inside nanotube shells are realized by applying bias voltages between 1.5 V and 2.5 V. The average mass flow rate of the copper was found to be 120 ag/s according to TEM video imaging (measured visually at approximately 11.6 nm/s through the CNT). Successful soldering of a copper-filled CNT onto another CNT using a nanorobotic manipulator shows promise for nano spot welding, which can play a role similar to its macro counterpart for the interconnection of nano building blocks for the assembly of nanoelectronic circuits and nanoelectromechanical systems (NEMS).**

I. Introduction

With the continuing development of bottom-up nanotechnology fabrication processes, spot welding may likewise play an important role in interconnecting carbon nanotubes (CNTs) [1], nanowires [2], nanobelts [3], nanohelixes [4, 5], and other nanomaterials and structures for the assembly of nanoelectronic circuits and nanoelectromechanical systems (NEMS).

Van der Waals forces [6], electron-beam-induced deposition (EBID) [7], focused-ion-beam chemical vapor deposition (FIB-CVD) [8], high-intensity electron-beam welding [9], and nanomechanochemical bonding [10] are experimentally demonstrated interconnection strategies, though all have limitations. Van der Waals forces are generally very weak, nanomechanochemical bonding [10] are promising but not yet mature, and the other methods involve high-energy electron or ion beams, which significantly limits their applications. Another interconnection approach is to use CNTs, with their hollow cores and large aspect ratios [11, 12] as possible conduits for nanoscale amounts of various materials that can be used to fuse CNTs together. A variety of materials have been encapsulated by CNTs such as metals and their compounds [13-18], water [11], and fullerenes [19], and applications of devices as templates [20], thermometers [21], and nano test tubes [22] have been presented. The possibility to deliver [23] encapsulated materials from the carbon shells is of great interest because of the potential applications as atomic sources for nanoprototyping, nanoassembly, and injection. Recently, novel CNTs filled with single crystalline Cu-nanoneedles have been synthesized by a thermal CVD method using alkali modified copper catalysts [24]. Because copper is a good conductor of heat and electricity and has a very low binding energy (0.1–0.144 eV/atom) when bound to carbon, encapsulated copper inside nanotubes is ideal for many of these potential applications. Here we present an experimental investigation of controlled melting and flowing of single crystalline copper from CNTs assisted by nanorobotic manipulation [6], and its application in spot welding of nanotubes using this copper.

Manuscript received September 15, 2006. This work is conducted with financial support from the ETH Zurich and the Chinese National Science Foundation (No. 50571087); the Hi-tech Research and Development Program of China (863) (2002 AA334020), the Natural Sciences Fund of Zhejiang Province (Y404274).

Lixin Dong, Li Zhang, and Bradley J. Nelson are with Swiss Federal Institute of Technology (ETH), Zurich, Switzerland, and Xinyong Tao and Xiaobin Zhang are with Zhejiang University, Hangzhou, China.

*Contacting Author: Bradley J. Nelson is with ETH-Zurich, (phone: +41 44 632-5529; fax: +41 44 632-1078; email: bnelson@ethz.ch).

II. System Setup

A. Concept of Nanorobotic Spot Welding

The concept of nanorobotic spot welding is schematically shown in Fig. 1. A metal-filled carbon nanotube is positioned with a nanorobotic manipulator to the interconnection site and the metal is then deposited to solder the nano building blocks, such as CNTs and nanowires, together, or to weld them onto electrodes. It can be understood that controlled metal deposition besides nanometer scale positioning will be a critical technique.

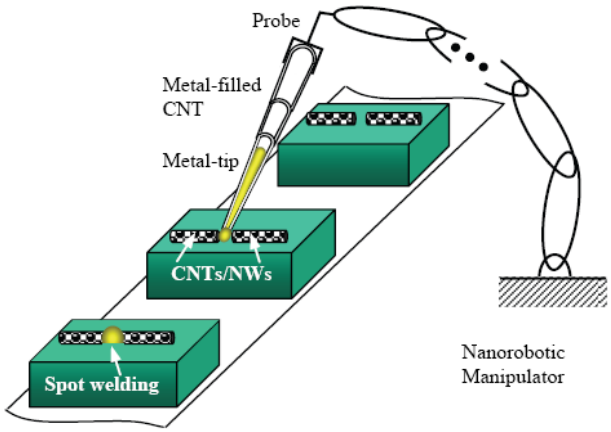

Fig. 1. Concept of nanorobotic spot welding.

B. Cu-filled Carbon Nanotubes

The CNT samples are synthesized using an alkali doped Cu catalyst by a thermal CVD method [24]. Figure 2a to c show their structures imaged by field-emission scanning electron microscopy (FESEM, Sirion, FEI), transmission electron microscope (TEM, JEM-2010, 200 kV), selected area electron diffraction (SAED) and high-resolution TEM (HRTEM). It can be seen from these observations that the yield of the Cu-filled CNTs is high. The CNTs are up to 5 μm long with outer diameters in a range of 40–80 nm. The single crystalline Cu nanoneedles are encapsulated in graphite walls approximately 4 to 6 nm thick in the first sections of the bamboo-structured CNTs. The graphite layers are not parallel to the tube axis.

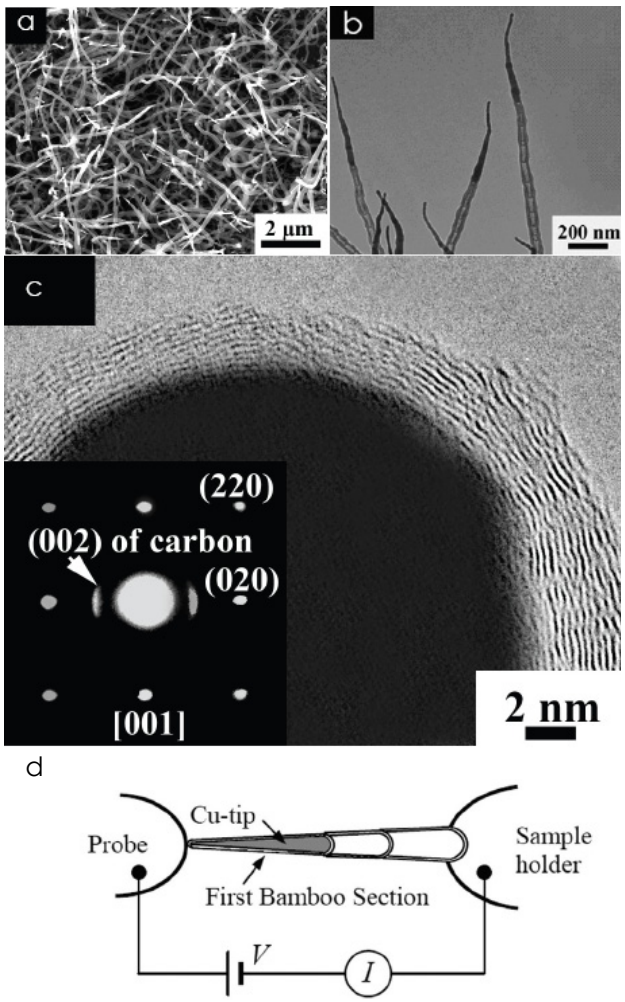

Fig. 2. (a to c) Copper-filled CNTs. (a) FESEM images of Cu filled CNTs. Observation shows that all the CNTs have sharp tips filled with metal nanoneedles. These CNTs are up to 5 μm long with outer diameters in a range of 40-80 nm. (b) TEM image of typical copper-filled CNTs synthesized for 30 min. (c) HRTEM image reveals that the Cu nanoneedles are encapsulated in graphite walls approximately 4-6 nm thick. The inset is the corresponding SAED pattern of the Cu nanoneedle along the [112] zone axis, showing that the Cu nanoneedle is single crystalline. The appearance of a pair of arcs in the SAED pattern indicates some orientation of the (002) planes in the carbon tubes. The interlayer spacing of carbon nanotube is about 0.34 nm, consistent with the (002) plane lattice parameter of graphite. It can also be seen that the graphite layers are not parallel to the tube axis. (d) Schematic setup of the probe of a nanorobotic manipulation system in a TEM, ST1000 STM-TEM holder (Nanofactory Instruments AB).

C. Nanorobotic Manipulators

Our experiments were performed in a CM30 TEM equipped with a scanning tunneling microscope (STM) built in a TEM holder (Nanofactory Instruments AB, ST-1000) serving as a manipulator as schematically shown in Fig. 2d. The material consisting of a CNT bundle is attached to a 0.35 mm thick Au wire using silver paint, and the wire is held in the specimen holder. The probe is an etched 10 μm thick tungsten wire with a tip radius of approximately 100 nm (Picoprobe, T-4-10-1mm). The probe can be positioned in a millimeter-scale workspace with sub-nanometer resolution with the STM unit actuated by a three-degree-of-freedom piezo-tube, making it possible to select a specific CNT. Physical contact can be made between the probe and the tip of a nanotube. Applying a voltage between the probe and the sample holder establishes an electrical circuit through a CNT and injects thermal energy into the system via Joule heating. By increasing the applied voltage, the local temperature can be increased past the melting point of the copper encapsulated in a tube. The process is recorded by TEM images and real-time video.

III. Controlled Melting and Delivery

Figure 3 shows TEM images of melting and flowing copper inside the carbon shells of a Cu-filled CNT. The tip of a Cu-filled CNT is first brought into contact with the tungsten probe (Fig. 3a). Then a bias voltage is applied on the two ends of the CNT with the tungsten probe serving as the anode. The voltage is slowly increased from 0 mV with 100 mV steps. When the voltage reaches 1500 mV, a vacant section inside the carbon shells appears, indicating that the copper has begun melting (Fig. 3b). Transportation of the copper to the probe-tip contact moves the vacant section to the root of the first bamboo section of the Cu-filled CNT (Fig. 3c). After the vacant section reaches the root, the copper core starts to flow to the tip of the CNT when bias is increased to 2500 mV. After all the copper flows out, the probe is moved away from the CNT while keeping the bias on (Fig. 3d). A sphere is visible on the tip of the CNT (see inset for a high magnification image) suggesting the formation is related to a melting process. Applying an image processing routine to the data from these experiments, we calculate that the Cu-filled section has an external diameter of approximately 52 nm at the root and 30 nm near the tip, whereas the original Cu core has a diameter of about 39 nm and 22 nm and a length of 874 nm. The diameter of the copper sphere is 49 nm. Therefore, we determine the mass of the original copper core is approximately 6 fg (femtograms) and the resulting sphere is 0.5 fg according to the density of copper (8.92 g cm^{-3}). We deduce that the missing mass (91%) diffused onto the tungsten probe.

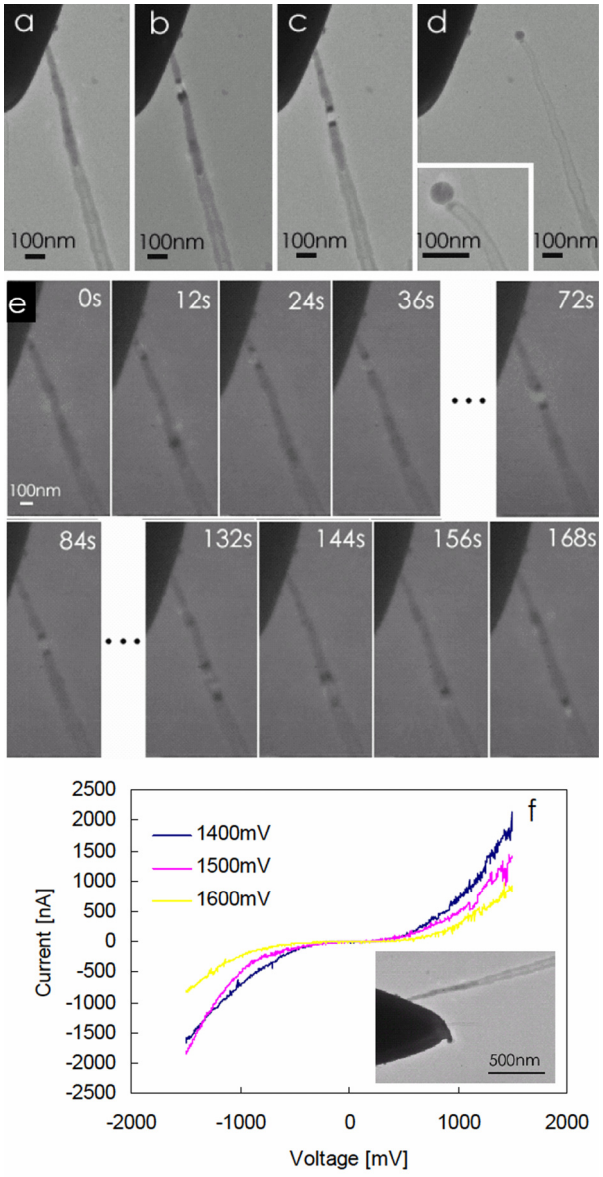

Fig. 3. TEM images of melting and flowing of copper inside carbon shells. (a) A Cu-filled CNT is brought into contact with a tungsten probe. (b and c) Under a 1.5 V bias, a vacant section appeared and moved to the root of the first bamboo section of the Cu-filled CNT showing the melting occurred. After then the copper starts to flow to the tip of the CNT under a 2.5 V bias. (d) After all the copper flows out, the probe is moved away from the CNT. A sphere is visible on the tip of the CNT (see inset for a high magnification image). The Cu-filled section has an external diameter of ca. 52 nm at the root and ca. 30 nm near the tip, whereas the Cu core has a diameter of ca. 39 nm and 22 nm, respectively. The diameter of the copper sphere is ca. 49 nm. (e) Time-resolved TEM images from video frames showing the melting process. The first vacant section (Fig. 3b) formed at 48 sec., and the second one (Fig. 3c) at 86 sec. The vacant section then moves to the bottom of the first bamboo section of the CNT. Obvious melting occurred when the bias voltage reaches 1500 mV from 0 mV with 100 mV steps. (e) Current vs. voltage curves are obtained during the process showing an obvious current drop at 1500 mV as melting began, which we attribute to resistance increases of the tube due to the increased temperature. It can also be seen that under -1500 mV, the current is larger that under -1400 mV, which could be a result of the decrease of the contact resistance between the nanotubes and the probe due to the flowed out of copper. Inset of (f) shows the configuration of I-V characterization.

The entire process was recorded with real time TEM imaging. Fig. 3e shows selected video frames of the melting process. The first vacant section (Fig. 3b) formed at 48 sec., and the second one (Fig. 3c) at 86 sec. The vacant section then moves to the bottom of the first bamboo section of the CNT. Current vs. voltage curves were obtained (Fig. 3f) during the process, showing an obvious current drop at 1500 mV as melting began, which we attribute to resistance increases of the tube due to increased temperature. It can also be seen that under -1500 mV, the current is larger than under -1400 mV, which could be a result of the decrease of the contact resistance between the nanotube and the probe due to the copper flowing from the tube onto the probe. This indicates that the originally closed caps of the CNTs are opened by a thermally induced increase in internal tube pressure.

The melting is due to Joule heating of the copper by the transport current and electron beam bombardment by the TEM. The irradiation of the electrons can cause the temperature increase of the sample due to inelastic scattering, but because of the low intensity of the beam and the short time, electron beam bombardment is not the main mechanism. Also, no melting or morphology changes of the copper core have been observed before applying the bias voltage, therefore, we attribute transportation current induced Joule heating to be the main factor. The current can be readily controlled by adjusting the external voltage, which makes this approach easily applied in NEMS since the process does not require involve a high energy beam source.

Figure 4a is a series of time-resolved TEM images taken from video frames showing the flowing process. The copper core started to flow inside the carbon shell from the bottom to the tip of the first bamboo section as the bias voltage reaches 2.5 V. The entire process continued for about 70 seconds. The flow rate was found to be 11.6 nm/s according to the change of apparent length of the copper core (Fig. 4b). Accordingly, we calculated the mass change as shown in Fig. 4b, and the mass flow rate can be then be determined by fitting the data to the curve $3\times10^{-9}t^2-1.2\times10^{-3}t+0.12$, yielding approximately 120 ag/s, which is strikingly slow and well controllable, allowing precise delivery of mass at attogram scale for time-based control can readily reach sub-second precision.

According to time-resolved current vs. voltage characteristics under a constant positive bias of 2.5 V, the current density under 2.5 V when flowing occurred is then calculated according to the cross sectional area as 2.60-3.07×10^6 A/cm^2. This is comparable to the observed value for electromigration of iron in CNTs (ca. 7×10^6 A/cm^2) [23]. The difference can be a result of the lower binding energy of copper to the carbon shells (0.1–0.144 eV/atom) than that of irons to carbon shells (0.3 eV/atom) [25]. The high current densities employed here will lead to resistive heating. Temperatures as high as 2000 to 3000 °C have been estimated according to the lattice spacing change in electric

breakdown experiments on non-filled multiwalled nanotubes (MWNTs) [26] at a slightly higher bias (3V) than those used here. We then correlated the current density J and the mass flow rate $\dot{m}$ as shown in Fig. 4c. The relation $\dot{m} = 0.3135J^2 - 1.6206J + 2.1373$ suggests that a real positive value of $\dot{m}$ ($\geq$ 42.9 ag/s) can only be given when the current density J surpasses 2.5847 $\times 10^6$ A/cm^2. The existence of this threshold also implies the mechanism of the observed flowing is most possibly electromigration [23]. Under a negative bias, i.e., when the tungsten probe serves as a cathode, we observed flow in the opposite direction.

Other possible mechanisms for flow can be excluded. Capillary force can induce filling/flowing, but the direction should be opposite to the observed flow, i.e., from the tip to the bottom of the carbon shells. Thermal expansion can enable flow, but the flow should be isotropic heading towards both the tip and the bottom. A recent investigation showed that the irradiation of MWNTs can cause a large pressure buildup within the nanotube core that can plastically deform, extrude, and break encapsulated solid material [27]. In our experiments, however, no contraction of the carbon shells was observed.

Figure 4d shows time-resolved resistance changes under 2.5 V as flowing occurred. The circuit resistance is composed of five parts shown schematically in the inset of Fig. 4d, i.e., the contact resistance between the copper tip and the probe R_{C1}, the resistance of the copper core R_{Cu}, the resistance of the first section of carbon shell without copper R_{CNT1}, the resistance of the other sections of the nanotubes R_{CNT2}, and the contact resistance between the CNT and the sample holder R_{C2}. Note that the carbon shell with a copper core is in fact shortened by the copper core. Hence, the measured resistance is $R = R_{C1} + R_{Cu} + R_{CNT1} + R_{CNT2} + R_{C2}$. At t = 0 s, the first section of the Cu-filled CNT has a copper core of 822.9 nm according to the fit value shown in Fig. 3b, so the total resistance will exclude the R_{CNT1}, i.e., $R_{t=0} = R_{C1} + R_{Cu} + R_{CNT2} + R_{C2}$. Similarly, at t = 70.9 s, the entire copper core flows out. In this case, the total resistance will exclude R_{Cu}, i.e., $R_{t=70.9s} = R_{C1} + R_{CNT1} + R_{CNT2} + R_{C2}$. According to the value fit in Fig. 4d, $R_{t=0s} = 59.38$ kΩ and $R_{t=70.9s} = 73.94$ kΩ. The difference (14.75 kΩ) equals the resistance of the full length of the carbon shell in the first section without copper and that of the full length copper core. Because the resistivity of copper (1.57×10^{-8} Ωm) is sufficiently smaller than that of CNTs (on the order of 10^{-6} Ωm) [28], it is reasonable to ignore the resistance of copper in the difference. Hence, we can extract the resistance of the carbon shells from the measured circuit resistance. The increase of the resistance along with the time is mainly caused by the shortening of the low resistant copper core and, accordingly, the continuous exposure of the high resistant carbon shells. The resistivity of the carbon shells can, thus, be

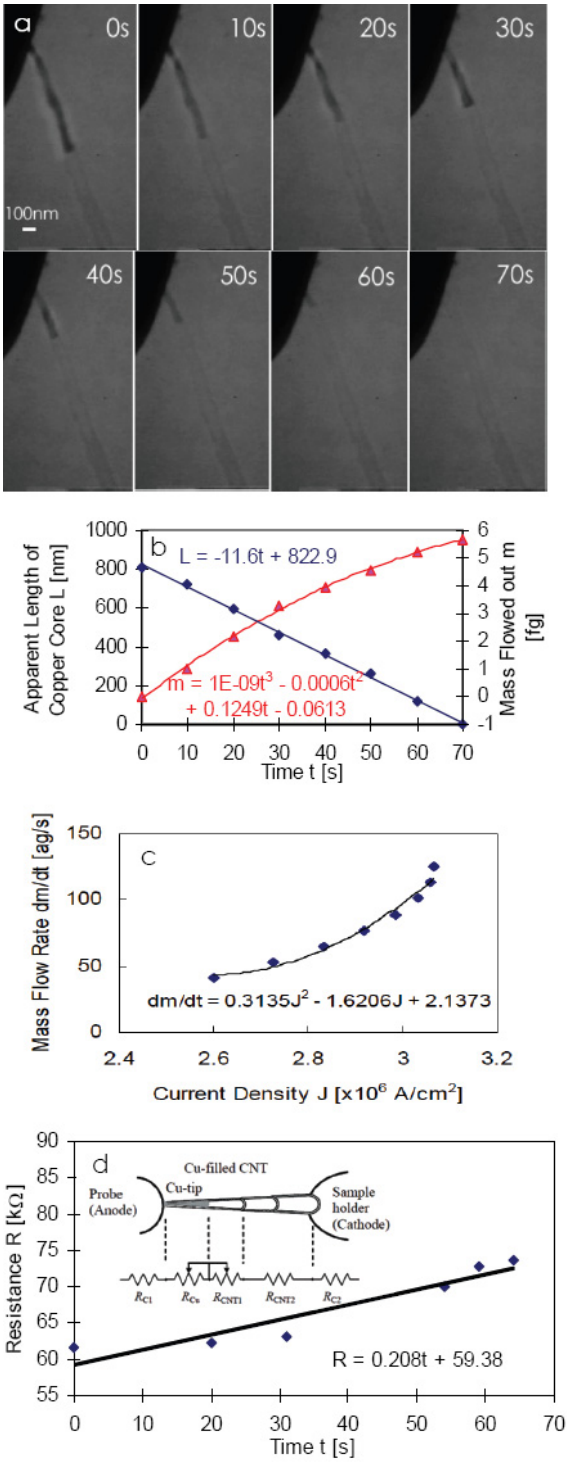

Fig. 4. (a) Time-resolved TEM images from video frames showing the flowing process. The copper core started to flow inside the carbon shells from the root to the tip as the bias voltage reaches up to 2.5 V. The whole process has continued for about 70 seconds. (b) The flow rate has been found to be 11.6 nm/s according to the change of apparent length of the copper core. The tungsten probe has been positively biased. The mass flow rate can be then drawn out from the fitting curve as approximately 0.12 fg/s. (c) Relation between the current density J and the mass flow rate $\dot{m}$. (d) Time-resolved resistance changes under 2.5 volts as flowing occurring. Inset shows the electric circuit model of the Cu-filled CNT.

worked out as 1.6 $\times 10^{-6}$ Ωm according to the resistance (14.75 kΩ) and the average cross area of the shell (91 nm^2). This is a value smaller than that of natural graphite (1.4×10^{-5} Ωm) [29] and four point measurements of supported, unfilled, MWNTs (9.0×10^{-6} Ωm) [28], suggesting that multiple layers have been involved in carrying the current because of the end contact established between the CNT tip and the tungsten probe. It should be noted that, though we used two-terminal measurement, the resistance of the carbon shells originally with copper inside has been successfully identified due to the flowing of the copper, which provides a new method for extracting the resistance of a component from a measured circuit resistance without involving four-terminal measurement. This is particularly useful for the investigation of hetero-structures such as metal-filled CNTs provide when they have sufficiently different resistivities and melting points. It can also be found that the absolute value of the current at 1.5 V is about one-order-of-magnitude larger than that shown in Fig. 3f, which can be assigned to the improvement of the contact resistance between the CNT-tip and the tungsten probe due to the melted copper. Though we have no way of measuring the actual temperature of the nanotubes or the copper core, this process provides the possibility for estimating the temperature according to the resistivity change if we apply Matthissen's rule on temperature dependence of resistivity provided we know the resistivity at a certain temperature. Unfortunately, the latter is unknown. However, it has been noted that the temperature for CNT growth from 100-nm scale Cu particles in our synthesis (700 ^{0}C) is far lower than the melting point of bulk Cu (1083 ºC) [24]. It is well known that the surface-to-volume ratio with respect to a nano-sized particle can affect the melting point. Though the exact reason for melting at such a low temperature is not yet known, we have a rough estimation of the melting point of the copper core, i.e., around 700 ºC. This is comparable to the *in situ* electron microscope observations of the melting point of the encapsulated 20–60 nm diameter Cu nanocrystals in multilayer graphitic carbon spheres, which was reported at 802 ºC [30]. We also know according to the experiment that the melting point of the carbon shells is much higher than that of the copper core. This provides further evidence of molten copper inside carbon shells.

IV. Nanorobotic Spot Welding

The application of such controlled transportation of the copper core is then investigated. Self-soldering of CNTs with copper encapsulated in a CNT is shown in Fig. 5. A copper-filled tube, CNT_1, is first attached to a tungsten probe (Fig. 5a). A section of CNT_1 is then attached to and soldered onto CNT_2 by the melted copper (Fig. 5b). Figures 5c-h are video frames showing the soldering process. A copper-filled tube, CNT_1, is attached to a probe, and brought into contact with another tube, CNT_2. The probe has a -10 V bias. Figures 5c-e show three different positions as the probe is approaching CNT_2. Figure 4f shows how contact has been made. The shape change of the copper suggested a melting process has occurred. It has been found from the video frames (25 fps) that the melting the copper happened in a very short interval (< 70ms). With a higher bias (-15 V), CNT_1 is broken (Fig. 5g) and its end section remains soldered to the tip of CNT_2 (Fig. 5h).

Compared with the other interconnection processes previously investigated, electrically driven spot welding has several interesting aspects. (i) A very low current can induce the melting and drive the flow; which is much more efficient that irradiation-based techniques involving high energy electron beams [7, 9, 27, 31, 32], FIB [8], or lasers [12]. Combined with dielectrophoretic assembly, it is possible to solder the tubes onto electrodes for batch fabrication of NEMS. (ii) The welding site can be readily selected using nanorobotic manipulation, which enables 3D position and orientation control for continuous mass delivery and will potentially enable 3D prototyping and assembly. (iii) The melting occurs rapidly (at least milli-second level); several orders-in-magnitude faster than that using high-intensity electron-beam or FIB, which is generally on the order of a

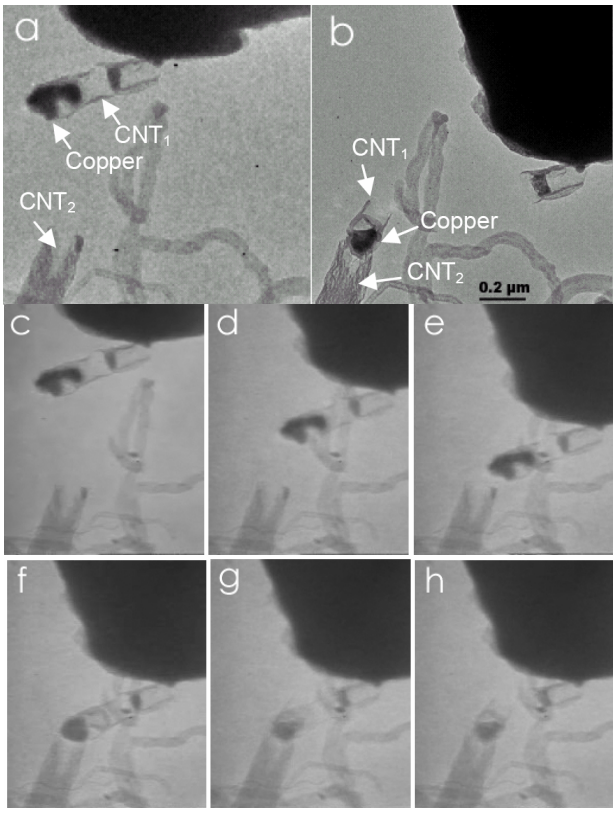

Fig. 5. Self-soldering of CNTs with copper encapsulated in a CNT. (a) A copper-filled tube, CNT_1, is attached to a tungsten probe. (b) A section of CNT_1 is soldered onto CNT_2 by the melted copper. (c to h) Video frames showing the soldering process. A copper-filled tube, CNT_1, is first attached to a probe, and brought into contact with another tube, CNT_2. The probe (cathode) has a -10 V bias. (c-e) Three different positions as the probe is approaching CNT_2. (f) shows how contact has been made. The shape change of the copper suggested a melting process has occurred. With a higher bias (-15 V), CNT_1 is broken (g) and its end section remains soldered to the tip of CNT_2 (h).

minute [7-9, 27, 32]. (iv) Because both the rate and direction of mass transport depends on the external electrical drive, precise control of an ultra-small mass delivery is possible. Time-based control will allow the delivery of attograms of mass [33]. (v) Copper has good compatibility in the conventional semiconductor industry. Our experiments show that it will likewise play an important role for scaled down systems. Carbon shells provide an effective barrier against oxidation and consequently ensure a long-term stability of the copper core, which also facilitates the conservation of the material than conveying mass on the external surface of nanotubes [33].

V. Conclusion

In summary, spot welding using single-crystalline-copper-filled CNTs has been investigated experimentally using nanorobotic manipulation inside a TEM. Controlled melting and flowing of copper inside nanotube shells have been realized by applying a bias voltage of as low as 1.5 and 2.5 V, respectively. The melting is a result of Joule heating, whereas the flowing is caused by electromigration. The flow rate of the copper has been found to be 11.6 nm/s under a 2.5 V bias using time-resolved TEM images, which is strikingly slow and well controllable, allowing precise delivery of mass. The mass flow rate has been determined to be 120 ag/s. A successful demonstration of self-soldering a copper-filled CNT onto another CNT shows promising for nano spot welding.

References

[1] S. Iijima, "Helical microtubules of graphitic carbon," *Nature,* vol. 354, pp. 56-58, 1991.

[2] A. M. Morales and C. M. Lieber, "A laser ablation method for the synthesis of crystalline semiconductor nanowires," *Science,* vol. 279, no. 5348, pp. 208-211, 1998.

[3] Z. W. Pan, Z. R. Dai, and Z. L. Wang, "Nanobelts of semiconducting oxides," *Science,* vol. 291, no. 5510, pp. 1947-1949, 2001.

[4] L. Zhang, E. Ruh, D. Grützmacher, L. X. Dong, D. J. Bell, B. J. Nelson, and C. Schönenberger, "Anomalous Coiling of SiGe/Si and SiGe/Si/Cr Helical Nanobelts," *Nano Lett.,* vol. 6, no. 7, pp. 1311-1317, 2006.

[5] D. J. Bell, L. X. Dong, B. J. Nelson, M. Golling, L. Zhang, and D. Grutzmacher, "Fabrication and characterization of three-dimensional InGaAs/GaAs nanosprings," *Nano Lett.,* vol. 6, no. 4, pp. 725-729, 2006.

[6] L. X. Dong, F. Arai, and T. Fukuda, "Destructive constructions of nanostructures with carbon nanotubes through nanorobotic manipulation," *IEEE/ASME Trans. on Mechatronics,* vol. 9, no. 2, pp. 350-357, 2004.

[7] L. X. Dong, F. Arai, and T. Fukuda, "Electron-beam-induced deposition with carbon nanotube emitters," *Appl. Phys. Lett.,* vol. 81, no. 10, pp. 1919-1921, 2002.

[8] S. Matsui, T. Kaito, J. Fujita, M. Komuro, K. Kanda, and Y. Haruyama, "Three-dimensional nanostructure fabrication by focused-ion-beam chemical vapor deposition," *J. Vac. Sci. Technol. B,* vol. 18, no. 6, pp. 3181-3184, 2000.

[9] S. Y. Xu, M. L. Tian, J. G. Wang, J. Xu, J. M. Redwing, and M. H. W. Chan, "Nanometer-Scale Modification and Welding of Silicon and Metallic Nanowires with a High-Intensity Electron Beam," *Small,* vol. 1, no. 12, pp. 1221-1229, 2005.

[10] L. X. Dong, F. Arai, and T. Fukuda, "Nanoassembly of carbon nanotubes through mechanochemical nanorobotic manipulations," *Jpn. J. Appl. Phys. Part 1,* vol. 42, no. 1, pp. 295-298, 2003.

[11] S. Supple and N. Quirke, "Rapid imbibition of fluids in carbon nanotubes," *Phys. Rev. Lett.,* vol. 90, no. 21, p. 214501, 2003.

[12] P. Kral and D. Tomanek, "Laser-driven atomic pump," *Phys. Rev. Lett.,* vol. 82, no. 26, pp. 5373-5376, 1999.

[13] P. M. Ajayan and S. Iijima, "Capillarity-Induced Filling of Carbon Nanotubes," *Nature,* vol. 361, no. 6410, pp. 333-334, 1993.

[14] S. C. Tsang, Y. K. Chen, P. J. F. Harris, and M. L. H. Green, "A Simple Chemical Method of Opening and Filling Carbon Nanotubes," *Nature,* vol. 372, no. 6502, pp. 159-162, 1994.

[15] P. M. Ajayan, C. Colliex, J. M. Lambert, P. Bernier, L. Barbedette, M. Tence, and O. Stephan, "Growth of Manganese Filled Carbon Nanofibers in the Vapor-Phase," *Phys. Rev. Lett.,* vol. 72, no. 11, pp. 1722-1725, 1994.

[16] C. Guerretpiecourt, Y. Lebouar, A. Loiseau, and H. Pascard, "Relation between Metal Electronic-Structure and Morphology of Metal-Compounds inside Carbon Nanotubes," *Nature,* vol. 372, no. 6508, pp. 761-765, 1994.

[17] A. A. Setlur, J. M. Lauerhaas, J. Y. Dai, and R. P. H. Chang, "A method for synthesizing large quantifies of carbon nanotubes and encapsulated copper nanowires," *Appl. Phys. Lett.,* vol. 69, no. 3, pp. 345-347, 1996.

[18] X. Y. Tao, X. B. Zhang, J. P. Cheng, F. Liu, Y. Li, and G. Van Tendeloo, "Controllable synthesis of novel one-dimensional carbon nanomaterials on an alkali-element-modified Cu catalyst," *Nanotechnology,* vol. 17, no. 1, pp. 224-226, Jan 2006.

[19] B. W. Smith, M. Monthioux, and D. E. Luzzi, "Encapsulated C-60 in carbon nanotubes," *Nature,* vol. 396, no. 6709, pp. 323-324, 1998.

[20] P. M. Ajayan, O. Stephan, P. Redlich, and C. Colliex, "Carbon Nanotubes as Removable Templates for Metal-Oxide Nanocomposites and Nanostructures," *Nature,* vol. 375, no. 6532, pp. 564-567, 1995.

[21] Y. H. Gao and Y. Bando, "Carbon nanothermometer containing gallium - Gallium's macroscopic properties are retained on a miniature scale in this nanodevice," *Nature,* vol. 415, no. 6872, pp. 599-599, 2002.

[22] D. Ugarte, A. Chatelain, and W. A. de Heer, "Nanocapillarity and chemistry in carbon nanotubes," *Science,* vol. 274, no. 5294, pp. 1897-1899, 1996.

[23] K. Svensson, H. Olin, and E. Olsson, "Nanopipettes for metal transport," *Phys. Rev. Lett.,* vol. 93, no. 14, p. 145901, 2004.

[24] X. Y. Tao, X. B. Zhang, J. P. Cheng, Z. Q. Luo, S. M. Zhou, and F. Liu, "Thermal CVD synthesis of CNTs filled with single-crystalline Cu nanoneedles at tips," *Diamond and Related Materials,* vol. 15, pp. 1271-1275, 2006.

[25] M. Weissmann, G. García, M. Kiwi, R. Ramírez, and C.-C. Fu, "Theoretical study of iron-filled carbon nanotubes," *Phys. Rev. B,* vol. 73, p. 125435, 2006.

[26] J. Y. Huang, S. Chen, S. H. Jo, Z. Wang, D. X. Han, G. Chen, M. S. Dresselhaus, and Z. F. Ren, "Atomic-scale imaging of wall-by-wall breakdown and concurrent transport measurements in multiwall carbon nanotubes," *Phys. Rev. Lett.,* vol. 94, no. 23, p. 236802, 2005.

[27] L. Sun, F. Banhart, A. V. Krasheninnikov, J. A. Rodrıguez-Manzo, M. Terrones, and P. M. Ajayan, "Carbon Nanotubes as High-Pressure Cylinders and Nanoextruders," *Science,* vol. 312, pp. 1199-1202, 2006.

[28] C. Schonenberger, A. Bachtold, C. Strunk, J. P. Salvetat, and L. Forro, "Interference and Interaction in multi-wall carbon nanotubes," *Applied Physics A-Materials Science & Processing,* vol. 69, no. 3, pp. 283-295, Sep 1999.

[29] *The CRC Handbook of Chemistry and Physics*. Cleveland, Ohio: Chemical Rubber Co.

[30] A. K. Schaper, F. Phillipp, and H. Hou, "Melting behavior of copper nanocrystals encapsulated in onion-like carbon cages," *J. Mater. Res.,* vol. 20, no. 7, pp. 1844-1850, 2005.

[31] D. N. Madsen, K. Molhave, R. Mateiu, A. M. Rasmussen, M. Brorson, C. J. H. Jacobsen, and P. Boggild, "Soldering of nanotubes onto microelectrodes," *Nano Lett.,* vol. 3, no. 1, pp. 47-49, 2003.

[32] T. Yokota, M. Murayama, and J. M. Howe, "In situ Transmission-Electron-Microscopy Investigation of Melting in Submicron Al-Si Alloy Particles under Electron-Beam Irradiation," *Phys. Rev. Lett.,* vol. 91, p. 265504, 2003.

[33] B. C. Regan, S. Aloni, R. O. Ritchie, U. Dahmen, and A. Zettl, "Carbon nanotubes as nanoscale mass conveyors," *Nature,* vol. 428, no. 6986, pp. 924-927, 2004.